NANOSYSTEMS:
PHYSICS, CHEMISTRY, MATHEMATICS

Smyslova V.G., et al. *Nanosystems: Phys. Chem. Math.*, 2024, **15** (6), 893–901.
http://nanojournal.ifmo.ru
DOI 10.17586/2220-8054-2024-15-6-893-901

Original article

Effect of nanostructuring of coprecipitated precursors on the morphology and scintillation properties of multication ceramics with a garnet structure

Valentina G. Smyslova[1,a], Vasiliy M. Retivov[1,b], Valery V. Dubov[1,c], Lidia V. Ermakova[1,d], Vladimir K. Ivanov[2,e], Petr V. Karpyuk[1,f], Ilya Yu. Komendo[1,g], Daria E. Lelekova[1,h], Vitaly A. Mechinsky[1,3,j], Andrey N. Vasil'ev[4,k], Artemii S. Ilyushin[4,l], Petr S. Sokolov[1,m], Mikhail V. Korzhik[1,3,n]

[1]National Research Center "Kurchatov Institute", Moscow, 123182, Russian Federation
[2]Kurnakov Institute of General and Inorganic Chemistry, Moscow, 119071, Russian Federation
[3]"Institute for Nuclear Problems" of the Belarusian State University, Minsk, 220030, Republic of Belarus
[4]Skobeltsyn Institute of Nuclear Physics, Moscow State University, Moscow, 119234, Russian Federation

[a]smyslovavg@gmail.com, [b]vasilii_retivov@mail.ru, [c]valery_dubov@mail.ru, [d]ermakova_lv@nrcki.ru, [e]van10@mail.ru, [f]karpyuk_pv@nrcki.ru, [g]komendo_iyu@nrcki.ru, [h]daria_kyznecova@inbox.ru, [j]vitaly.mechinsky@gmail.com, [k]anv@sinp.msu.ru, [l]artyom2833@mail.ru, [m]sokolov_ps@nrcki.ru, [n]korjikmikhail@gmail.com

Corresponding author: V. G. Smyslova, smyslovavg@gmail.com, smyslova_vg@nrcki.ru

PACS 81.20.Ev; 82.40.Qt

ABSTRACT Single-phase polycrystalline samples of the $(Gd,Y)_3Al_2Ga_3O_{12}$:Ce,Tb composition with a garnet structural type were obtained. Using various approaches to the preparation of the initial powders of hydroxycarbonate precursors and compaction methods, the grain size of the ceramics was varied. The scanning electron microscopy method was used to establish the features of the microstructure of the initial powders with different processing temperatures and the microstructure of the resulting ceramics. It is shown that an increase in the grain size of the ceramics and a decrease in the residual porosity gives a noticeable increase in optical transparency in the visible region of the spectrum, in which Ce^{3+} and Tb^{3+} ions emit during scintillation. The effect of intergrain boundaries of the ceramics on the diffusion features of nonequilibrium carriers, electrons and holes, as well as excitons formed during the absorption of ionizing radiation on the scintillation yield and energy resolution is considered.

KEYWORDS precursor, ceramics, garnet, microstructure, scintillation, light yield.

ACKNOWLEDGEMENTS Calculations of the dependence of the fluctuation contribution to the energy resolution of a crystalline scintillator on the grain size, the development of a scheme for the recombination of electrons and holes with the formation of charge-transfer excitons in a homogeneous crystal and in ceramics were obtained with the financial support of the Russian Federation represented by the Ministry of Education and Science of Russia, agreement No. 075-15-2021-1353 dated October 12, 2021. Research was done using equipment of "Research Chemical and Analytical Center NRC "Kurchatov Institute" Shared Research Facilities.

FOR CITATION Smyslova V.G., Retivov V.M., Dubov V.V., Ermakova L.V., Ivanov V.K., Karpyuk P.V., Komendo I.Yu., Lelekova D.E., Mechinsky V.A., Vasil'ev A.N., Ilyushin A.S., Sokolov P.S., Korzhik M.V. Effect of nanostructuring of coprecipitated precursors on the morphology and scintillation properties of multication ceramics with a garnet structure. *Nanosystems: Phys. Chem. Math.*, 2024, **15** (6), 893–901.

1. Introduction

Crystalline materials of the garnet structural type are widely used in various fields of photonics, especially in solid-state lasers [1] and in ionizing radiation detectors as scintillators [2]. Compounds of the garnet structural type based on triply charged cations have the space group $Ia-3d$ (#230, O_{10}^h), and their general formula can be represented as $C_3[B]_2(A)_3O_{12}$, where the C position and the positions in brackets, [] and (), correspond to cations in three different oxygen coordinations: distorted dodecahedral, octahedral and tetrahedral, respectively. Rare earth ions are localized in dodecahedral positions. Further progress in improving their consumer properties is associated with the complication of the cationic composition [3]. The use of garnet isomorphism is an exceptional opportunity to obtain multicomponent compounds of this structural type. The high tolerance of the garnet crystal lattice allows a wide variation of the elemental composition. Isovalent substitution is provided by changing the corresponding length of the metal-oxygen bond, which affects the luminescent properties of rare earth ions and is an additional tool for restructuring their spectral-luminescent

properties. The most significant results in the field of scintillators were obtained for gadolinium-aluminum-gallium garnets $Gd_3Al_2Ga_3O_{12}$ (GAGG), in which the [] and () positions are mixed with Al^{3+} and Ga^{3+} ions, and the Gd^{3+} ions either completely occupy dodecahedral positions in the lattice or are partially diluted with lanthanide or yttrium ions. Such materials are obtained by drawing from a melt [4–8] or by micro-pulling down method [9], and also in the form of ceramics by hot pressing [10, 11].

The listed methods require either expensive tooling made of platinum group metals or expensive equipment for high pressure sintering. To obtain transparent GAGG or more complex materials based on it, ceramic technology is of particular importance. Its advantages include obtaining the product without the stage of melting the precursor, which significantly minimizes the problem of defect formation in it due to evaporation at high temperatures and the difference in the pressure of saturated vapors of different components of the batch in the synthesis chamber. Ceramics of complex compounds can be obtained from a premix of simpler compounds of the same structural type [12], which allows controlling the spatial distribution of activator ions in the grains of the ceramics. Finally, hot pressing is not an exclusive approach to obtaining transparent ceramics of garnet compounds; it can also be obtained as a result of annealing in an oxygen atmosphere using nanoscabe precursors to obtain raw materials [13–17].

Nanostructuring of precursors in the technology of ceramics of the GAGG family of compounds allows solving two important problems: minimizing the evaporation of gallium from the compound and thereby maintaining a composition close to the specified one [18] and increasing the rate of compaction of the raw material during sintering due to the high reactivity of the precursor particles, which have a well-developed surface.

In this paper, it is shown that the use of co-precipitated nanoscale precursors of complex garnet compounds containing more than three cations allows us to solve a number of chemical engineering problems in the production of transparent scintillation ceramics. In particular, it is shown that ensuring a given composition of the compound with high accuracy at the stage of preparing the precursor for further pressing and sintering provides the ability to effectively adjust the scintillation properties by controlling the compositional disordering of the crystalline matrix.

2. Obtaining precursors of multicationic compounds by the coprecipitation method

The hydroxycarbonate precursor of following compositions $Gd_3Al_2Ga_3O_{12}$ (GAGG:Ce) and $(Gd,Y)_3Al_2Ga_3O_{12}$:Ce, Tb (GYAGG:Ce,Tb) were synthesized by co-precipitation from a mixed nitric acid solution containing Gd, Y, Ce, Tb, Al, and Ga. The following were used as feedstock materials: Gd_2O_3 (99.995%), Y_2O_3 (99.995%), AlOOH (99.998%), Ga (99.999%), $Ce(NO_3)_3$ $6H_2O$, and $Tb(NO_3)_3$ $6H_2O$ (99.95%). The feedstock of the main components was dissolved in the nitric acid of special purity grade 18-4, and the feedstock of the activators $Ce(NO_3)_3$ $6H_2O$ and $Tb(NO_3)_3$ $6H_2O$ was dissolved in deionized water (specific resistance 18 MOhm$\times$cm). Solutions of individual metals with known concentrations determined gravimetrically were mixed in the required ratio and diluted with water to a total metal concentration of 1 mol Me/l. The mixed solution was then gradually added to a solution of the ammonium hydrocarbonate NH_4HCO_3 with a concentration of 1.5 mol/l under constant stirring with an overhead stirrer. The resulting precipitate was filtered through a Buchner funnel, washed with a mixture of water and isopropanol, and dried for 6 h at 100 °C in a drying cabinet with forced convection. The precursor thus obtained was then subjected to heat treatment in a muffle furnace at temperatures above 600 °C for 2 h to convert it to the oxide form and form a garnet phase ($\geq$900 °C).

The completeness of precipitation was assessed using the inductively coupled plasma mass spectrometry (ICP-MS) method using a Perkin Elmer Elan DRC-e spectrometer. For this purpose, the content of the metals in the mother liquor and washing liquid determined, and the proportion of elements that did not precipitate relative to their initial amount in the mixed solution was calculated based on the data obtained. The analysis results for 10 syntheses are presented in Table 1.

TABLE 1. Completeness of precipitation during the synthesis of the GYAGG:Ce,Tb precursor

Element	The proportion of the element that did not pass into the sediment, % of the initial amount
Al	$< 0,02$
Ga	0,31±0,04
Y	0,10±0,02
Ce	$< 0,02$
Gd	$< 0,02$
Tb	$< 0,02$

The amounts of the elements which were not precipitated are within narrow limits that allows take them into account when planning syntheses and preparing mixed solutions. This ensures the preservation of the specified composition of the precipitate and the oxide with the garnet structure obtained from it, as well as the reproducibility of the syntheses.

The temperature of the garnet phase formation was estimated using differential scanning calorimetry (DSC) data. Fig. 1 shows the DSC results obtained on a TA Instruments SDT Q 600 at a heating rate of 10 °C/min, and the weight loss according to thermogravimetry (TG) data.

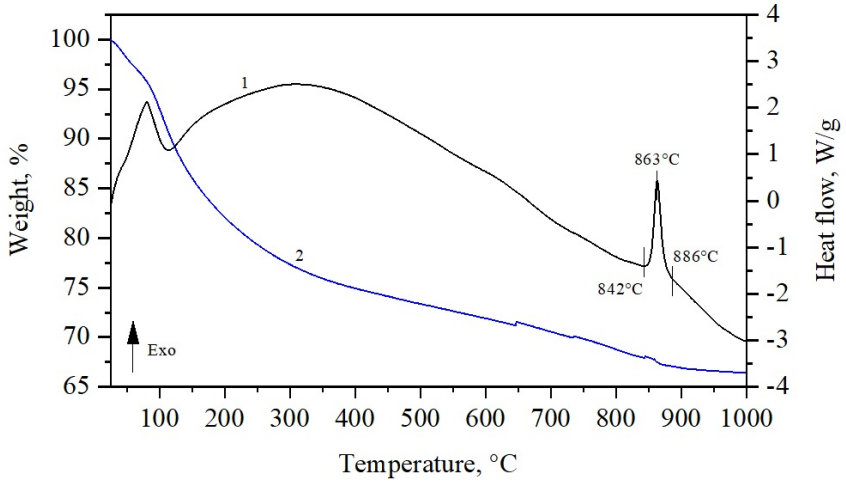

FIG. 1. TG (left axis) and DSC (right axis) curves of the GYAGG:Ce,Tb precursor: 1 – differential curve, 2 – mass loss curve

Solid samples treated at different temperatures for 2 h were analyzed by X-ray diffraction (XRD) on a BRUKER D2 PHASER diffractometer (CuK_α radiation, 2θ angle range from 15 to 95°, 0.02° step, Bragg-Brentano geometry) at room temperature. The results are shown in Fig. 2.

XRD data show that the samples are X-ray amorphous when annealed at temperatures up to 700°C. The cubic garnet phase ($Ia-3d$) is already formed and becomes predominant when the samples are annealed at 850 °C, which is close to the exothermic peak on the DSC curve. Its content is about 92 vol.%, and the remaining 8 vol.% is the impurity phase with the hexagonal perovskite structure *P63/mmc*. The reflections of these impurity phases are not observed in the diffraction pattern of the samples obtained at 900 °C. The low temperature of the garnet phase formation achieved in this production method allows reducing the evaporation of gallium oxide [19] during annealing, which ensures the production of single-phase samples with a given elemental composition.

Figure 3 shows the results of the study of the powder microstructure obtained on a Jeol JSM 7100 F scanning electron microscope (secondary electron mode, accelerating voltage 10 kV).

It is noticeable that the microstructure of the precursor and oxide powder does not undergo significant changes in the considered temperature range. This serves as additional confirmation of the uniform distribution of components at the level of nanosized primary particles.

The grain size of the final ceramics may depend on various factors. In particular, the structural features of the original powder or the presence of special additives - fluxes - may have an impact. Fig. 4 shows photo images and scanning electron microscopy images for ceramic samples of the GYAGG:Ce,Tb composition.

It can be seen that a significant increase in the grain size of ceramics and an increase in its optical transparency can be achieved by using a mixture of powders with different heat treatment temperatures during the production of ceramics: 850 and 1500 °C, respectively (Fig. 4, b, d). The grain size of the ceramics increases from an average value of 1 μm to 5 μm. A similar effect can be achieved by adding a sintering additive SiO_2 to the powder in an amount of 0.01 wt.% (Fig. 4, c, e), however, a certain heterogeneity in the grain size and a noticeable number of closed pores are observed, which may be associated with a sharp increase in the grain size during the sintering process. Thus, using a nanostructured precursor, it becomes possible to apply various approaches to control the morphology of ceramics.

Using the 3D printing method – stereolithography – it is possible to obtain ceramic elements of complex shape [20]. This method significantly expands traditional ceramic approaches, such as semi-dry pressing (compacting) and slip casting. Objects of complex geometry, such as openwork and mesh structures, are created due to controlled and local layer-by-layer polymerization of a photocurable suspension with ceramic particles when exposed to ultraviolet radiation. The composition of photocurable suspensions suitable for 3D printing consists of a mixture of the ceramic powder, low-viscosity acrylate monomer, UV photoinitiator and dispersing additive. We used 1,6-hexanediol diacrylate as an acrylate monomer. Another important advantage of this method is the relative availability of source materials for the preparation of suspensions and the low cost of modern desktop printers. After manufacturing by stereolithography, the green body – a

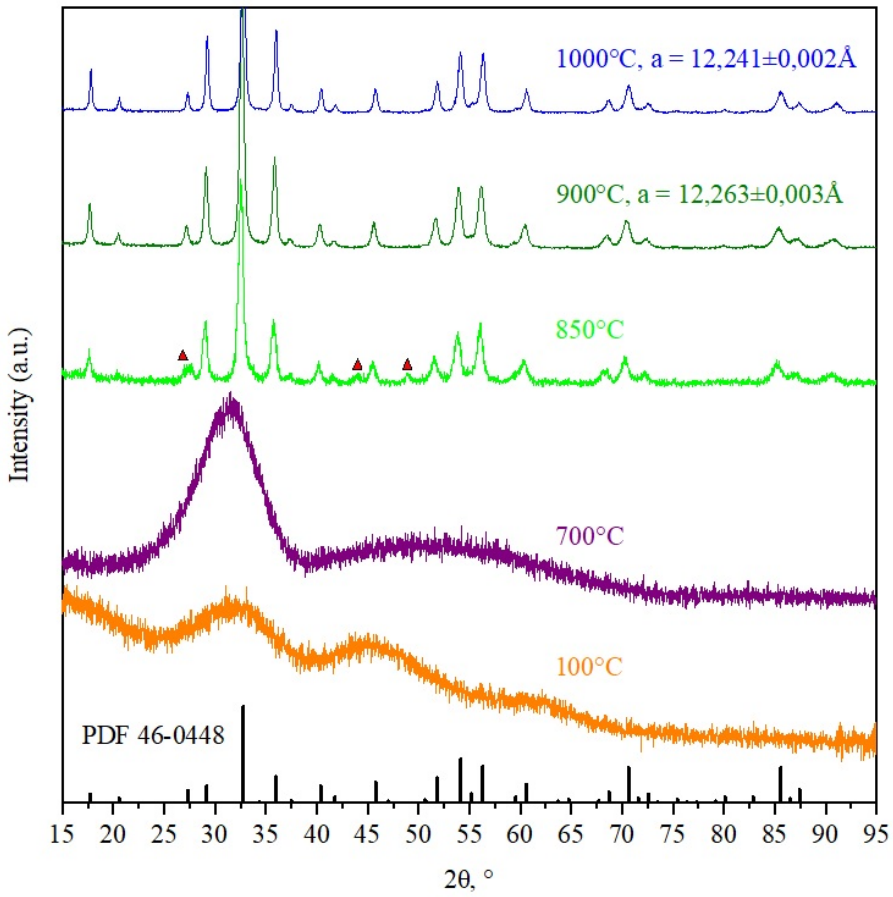

FIG. 2. Results of XRD analysis of the precursor and oxide powders GYAGG:Ce,Tb. Red triangles mark reflections related to the impurity phase

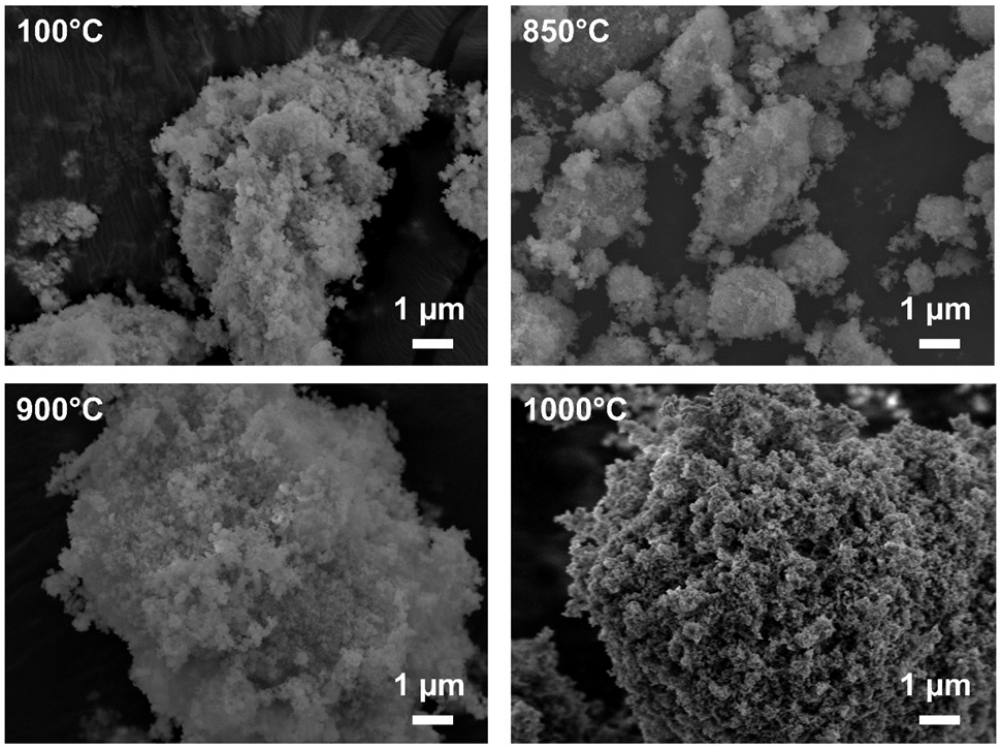

FIG. 3. SEM images of precursor and oxide powders of GYAGG:Ce,Tb after heat treatment at 100–1000 °C

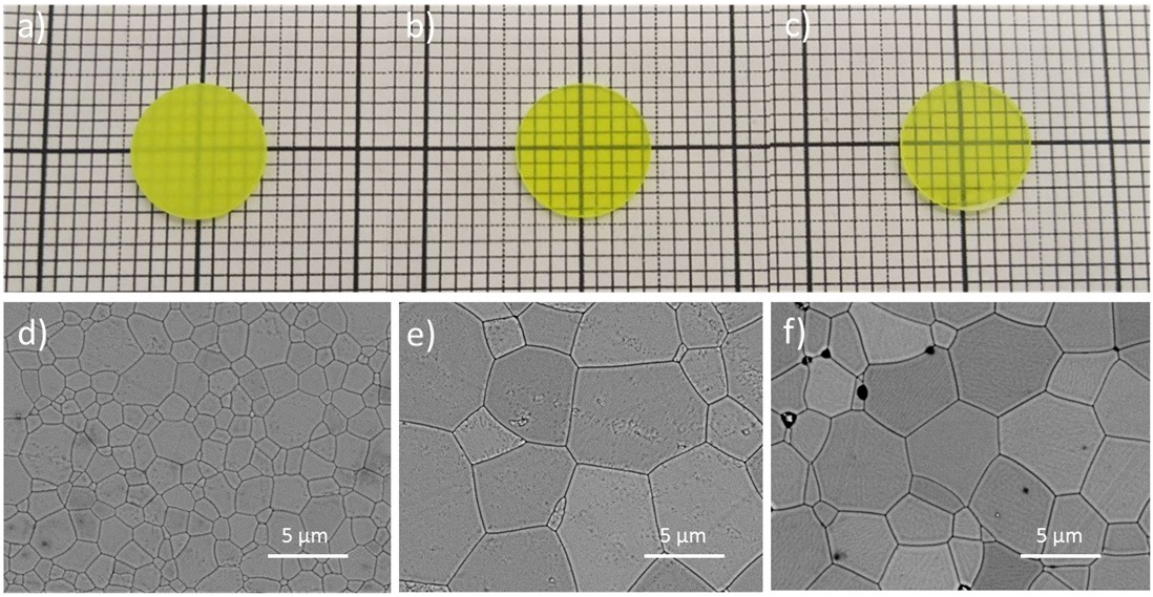

FIG. 4. Photographs and SEM images of GYAGG:Ce,Tb ceramic samples based on powder with a heat treatment temperature of 850 °C (a, d), based on a mixed powder of 850 °C + 1500 °C (b, e) and powder with heat treatment at 850 °C and the addition of 0.01 wt.% SiO_2 (c, f)

composite consisting of an acrylate polymer with encapsulated ceramic particles – requires burning out the organic binder and high-temperature sintering. These two operations are standard for the ceramic approach in general, but in the case of stereolithography, burning out in an inert atmosphere is usually required to remove the organic components from the green body without defects. A typical appearance of green bodies and ceramics of multicomponent garnets activated by cerium is shown in Fig. 5.

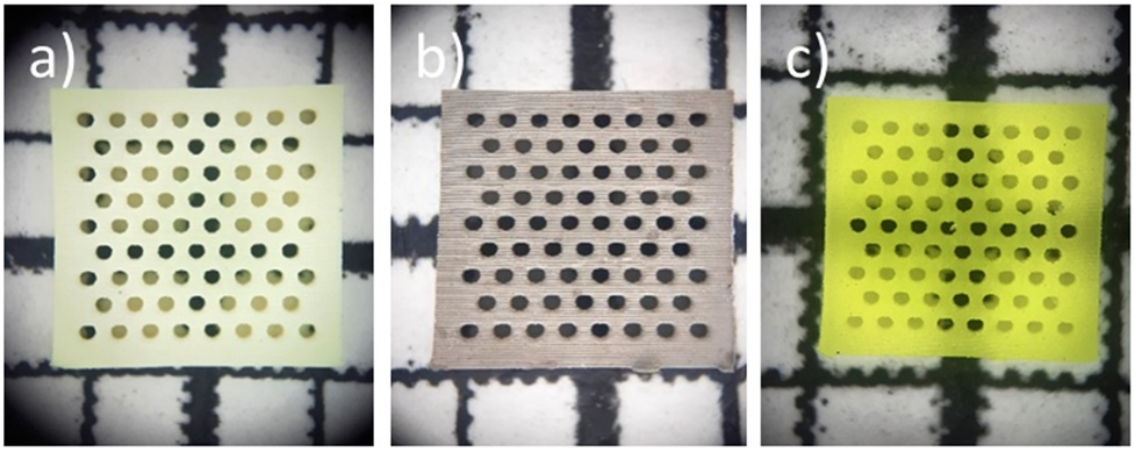

FIG. 5. Typical appearance of GYAGG:Ce,Tb raw materials after 3D printing (a), after burning out the organic binder (b) and high-temperature sintering (c) into dense oxide ceramics. The ceramic surfaces are not polished

Using the stereolithography method, it is possible to produce planar periodic structures from ceramics with a garnet structure.

3. Discussion of the results

The obtained data show that the morphology of transparent ceramics can vary significantly: the average grain size can vary from a few microns to more than 10 microns. Therefore, the question of the dependence of the scintillation parameters on the morphology of the ceramics, in particular, the grain size, is natural. From the point of view of the development of the scintillation process, ceramics differs from a single-crystal material by a number of factors. Firstly, a violation of the spatial periodicity of the crystal occurs at the boundaries between the grains and, as a consequence, nonequilibrium electrons and holes formed by ionizing radiation are additionally scattered at this boundary. In addition,

potential barriers to the movement of carriers may appear. Grain boundaries, clearly visible using scanning microscopy, can act as such energy barriers. The height of such barriers to the movement of electrons should not exceed the work function of the electron exit from the crystal into vacuum and depends on the orientation of the axes of the basis vectors of neighboring crystallites, and their spatial width depends on how tightly the ceramic grains fit together, that is, on the presence of pores in the ceramics. It can be assumed that electrons, holes and excitons can diffuse inside the grain with the same diffusion coefficients as in the crystal, but can move from one grain to another only due to slow tunneling processes. The boundary between the grains is a defect layer on which carriers can be captured and undergo nonradiative recombination. Finally, the grain boundary is enriched with the activator due to the large radius of the cerium ions Ce^{3+}. In this case, cerium at the boundary is predominantly in the state Ce^{4+} [21].

Let us consider some of the consequences of this difference. The elementary acts of fast electron scattering and the Auger processes for a hole in crystalline and ceramic samples do not differ from each other. In this regard, the structure of the track before thermalization will be the same in the crystalline and ceramic samples. The cascade of electron excitation multiplication ends when all secondary electrons and holes have an energy below the multiplication threshold (of the order of the band gap). Thus, in the garnets under consideration, by the end of multiplication, the electrons and holes will be distributed over kinetic energy within the range from zero to approximately 6 eV. Further relaxation is associated with the emission of optical phonons, as a result of which the electrons and holes fly away from their birthplace due to the hot diffusion process [22]. The average distance over which hot charge carriers fly away in the parabolic zone model increases with increasing initial energy E_{kin} of secondary electrons as $E_{kin}^{3/2}$. In oxide crystals with a typical optical phonon energy of about 100 meV, electrons with an energy of about 5 eV fly away from their birthplace on average by l_{term} ~30 nm, with the main flight occurring while their energy is sufficiently high (about 1 eV) [23]. Due to this, such electrons can fly over the intergranular barrier and enter the neighboring grain if they are born in a layer of thickness l_{term} near the intergranular boundary (the fraction of such electrons is about l_{term}/d, where d is the typical grain size). After thermalization, their return to the grain in which they were born and in which the hole remains is hindered by the presence of barriers. Thus, the number of electrons and holes born by the primary ionizing particle in different grains is not the same. If we assume that N_e electrons and N_h holes remain inside the grain, then the maximum number of excitons created by them should not exceed $\mathrm{Min}(N_e, N_h)$. This creates additional fluctuations in the number of generated electrons and holes due to the unequal number of carriers of different signs in the grains. As the grain size decreases, these fluctuations increase. Fig. 6 shows the dependence of this fluctuation contribution to the energy resolution of a crystalline element obtained by dividing the track of a primary electron with energy of 50 to 400 keV after thermalization into cells (grains) depending on the grain size. The simulation was carried out based on 100 (for 400 keV) to 800 (for 50 keV) generated tracks in a GAGG crystal. The simulation algorithm is described in [24]. It is evident that with an average grain size of ~5 μm, the contribution does not exceed 0.2%, i.e. it becomes insignificant. For small energies the contribution increases when the track length is about the grain size.

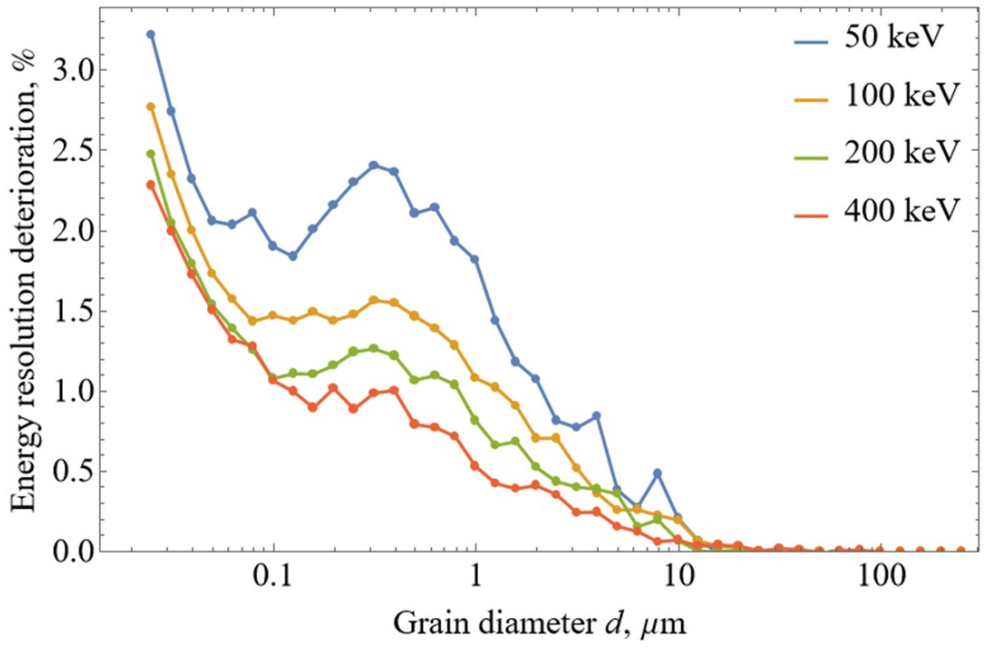

FIG. 6. Additional contribution to the energy resolution of a ceramic scintillator due to the difference in the numbers of electrons and holes in ceramic grains depending on the grain size. For a primary electron with an energy labeled in legend in GAGG

Assuming that all electrons and holes in the grains are bound into excitons, the yield of the ceramic scintillator should decrease compared to the crystalline one, since unpaired electrons and holes remain in the grains (over time, due to the long process of tunneling through barriers and due to capture by defects, including intergranular ones, these uncompensated charge carriers also recombine).

In a homogeneous crystal, during the process of diffusion-controlled recombination of an electron-hole pair, not all electrons and holes generated in one scattering event and located at a distance of the order of l_{term} from each other recombine, but only their share of the order of Min(1,R_c/l_{term}) [25, 26]. Here, the capture radius R_c is approximately equal to the Onsager radius – the distance at which the potential energy of attraction of an electron and a hole is of the order of thermal energy (at room temperature, the typical value of R_c is approximately 6–10 nm). The remaining electrons fly far from the hole and do not return to it, being captured by defects or recombining with "foreign holes" (in the region where the concentration of charge carriers is sufficiently high). On the other hand, if the electron thermalization occurs in the same grain in which it was born, it has a lower probability of moving away from the hole at a large distance, and thus the probability of its recombination with the hole increases. These processes are shown schematically in Fig. 7.

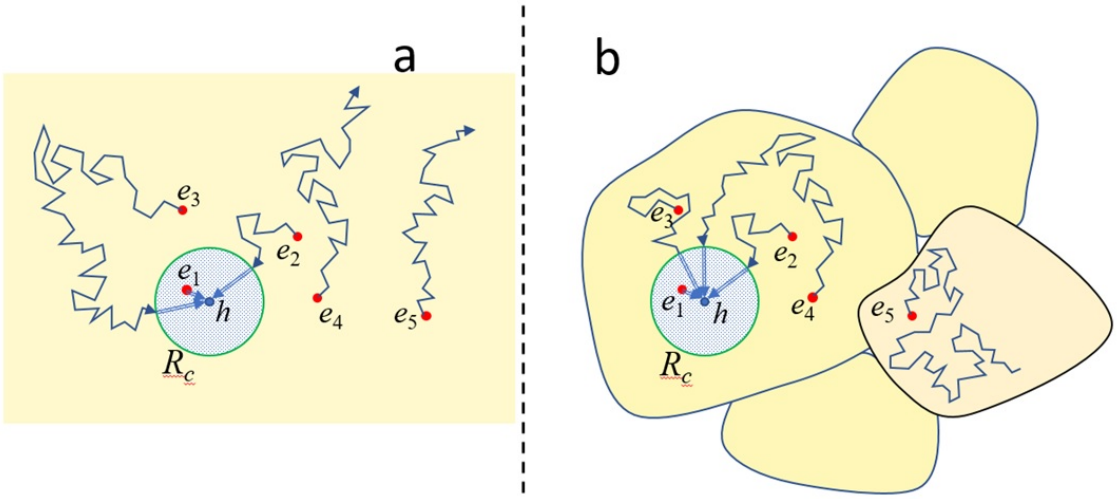

FIG. 7. Scheme of diffusion-controlled recombination of electrons and holes with the formation of charge-transfer excitons in a homogeneous crystal (a) and in ceramics (b)

The sphere of electron capture by a hole has a radius R_c (about 10 nm). Various cases of the location of a thermalized electron relative to a hole are shown (Fig. 7). Electron e_1 quickly recombines with the hole to form a charge-transfer exciton, electron e_2 recombines after a short diffusion, electron e_3 in a crystal recombines after a long diffusion in the crystal, and in ceramics its diffusion is limited by the grain size, and it enters the capture sphere faster. In a crystal, electrons e_4 and e_5 escape genetic recombination and can then recombine with other holes or be captured by defects. In ceramics, electron e_4 will recombine with a hole due to the diffusion region being limited by grain boundaries, and electron e_5 will be captured by another grain.

Due to the limitation of the scattering of electrons and holes, the yield of a ceramic scintillator can exceed the yield of a crystalline scintillator, despite the appearance of uncompensated electrons and holes in the grains. However, this also changes the kinetics of scintillations, in particular, the proportion of slow components decreases if they arise in the crystal due to the long migration of electron excitations over distances exceeding the grain sizes in the ceramics.

4. Conclusion

The influence of precursor morphology and sintering conditions on the characteristics of four-cation scintillation ceramics $(Gd,Y)_3Al_2Ga_3O_{12}$:Ce,Tb was analyzed. It was found that the grain size in transparent ceramics can vary within fairly wide limits. At the same time, it was found that the effects associated with the influence of grain boundaries on scintillation parameters become insignificant at grain sizes of ∼3–5 μm and above.

References

[1] Kaminskii A.A. *Laser crystals: their physics and properties*. Springer Ser. Opt. Sci., 1990, P. 214.
[2] Gektin A., Korzhik M. *Inorganic scintillators for detector systems*. Berlin: Springer, 2017, P. 20-77.
[3] Retivov V., Dubov V., Komendo I., Karpyuk P., Kuznetsova D., Sokolov P., Talochka Y., Korzhik M. Compositionally disordered crystalline compounds for next generation of radiation detectors. *Nanomaterials*, 2022, **12**(23), P. 4295.
[4] Kamada K., Endo T., Tsutumi K., Yanagida T., Fujimoto Y., Fukabori A., Yoshikawa A., Pejchal J., Nikl M. Composition engineering in cerium-doped $(Lu,Gd)_3(Ga,Al)_5O_{12}$ single-crystal scintillators. *Cryst. Growth Des.*, 2011, **11**(10), P. 4484–4490.
[5] Kamada K., Yanagida T., Pejchal J., Nikl M., Endo T., Tsutumi K., Fujimoto Y., Fukabori A., Yoshikawa A. Scintillator-oriented combinatorial search in Ce-doped $(Y,Gd)_3(Ga,Al)_5O_{12}$ multicomponent garnet compounds *J. Phys. D: Appl. Phys.*, 2011 **44**(50), P. 505104.

[6] Kamada K., Yanagida T., Endo T., Tsutumi K., Usuki Y., Nikl M., Fujimoto Y., Fukabori A., Yoshikawa A. 2 inch diameter single crystal growth and scintillation properties of Ce:$Gd_3Al_2Ga_3O_{12}$. *J. Cryst Growth*, 2012, **352**(1), P. 88–90.
[7] Kurosawa S., Shoji Y., Yokota Y., Kamada K., Chani V., Yoshikawa A. Czochralski growth of $Gd_3(Al_{5-x}Ga_x)O_{12}$ (GAGG) single crystals and their scintillation properties. *J. Cryst. Growth*, 2014, **393**, P. 134–137.
[8] Korzhik M., Alenkov V., Buzanov O., Dosovitsky G., Fedorov A., Kozlov D., Mechinsky V., Nargelas S., Tamulaitis G., Vaitkevicius A. Engineering of a new single-crystal multi-ionic fast and high-light-yield scintillation material $(Gd_{0.5}–Y_{0.5})_3Al_2Ga_3O_{12}$:Ce,Mg. *CrystEngComm*, 2020, **22**(14), P. 2502–2506.
[9] Sakthong O., Chewpraditkul W., Pattanaboonmee N., Chewpraditkul W., Yamaji A., Kamada K., Nikl M. Light yield and timing characteristics of $Lu_{0.8}Gd_{2.2}(Al_{5-x}Ga_x)O_{12}$: Ce,Mg single crystals. *IEEE Transactions on Nuclear Science*, 2020, **67**(10), P. 2295–2299.
[10] Seeley Z., Cherepy N., Payne S. Expanded phase stability of Gd-based garnet transparent ceramic scintillators. *J. Mater. Res.*, 2014, **29**(19), P. 2332–2337.
[11] Cherepy N., Kuntz J., Roberts J., Hurst T., Drury O., Sanner R., Tillotson T., Payne S. Transparent ceramic scintillator fabrication, properties, and applications. *Proc. SPIE*, 2008, **7079**, P. 263–268.
[12] Smyslova V., Kuznetsova D., Bondaray A., Karpyuk P., Korzhik M., Komendo I., Pustovarov V., Retivov V. and Tavrunov D. Advances of the cubic symmetry crystalline systems to create complex, bright luminescent ceramics. *Photonics*, 2023, **10**(5), P. 603.
[13] Luo Z., Jiang H., Jiang J. Synthesis of cerium-doped $Gd_3(Al,Ga)_5O_{12}$ powder for ceramic scintillators with ultrasonic-assisted chemical coprecipitation method. *J. Am. Ceram. Soc.*, 2013, **96**(10), P. 3038–3041.
[14] Drozdowski W., Witkowski M., Solarz P., Głuchowski P., Głowacki M., Brylew K. Scintillation properties of $Gd_3Al_2Ga_3O_{12}$:Ce (GAGG:Ce): a comparison between monocrystalline and nanoceramic samples. *Opt. Mater.*, 2018, **79**, P. 227–231.
[15] Yang S., Sun Y., Chen X., Zhang Y., Luo Z., Jiang J., Jiang H. The effects of cation concentration in the salt solution on the cerium doped gadolinium gallium aluminum oxide nanopowders prepared by co-precipitation method. *IEEE Trans. Nucl. Sci.*, 2014, **61**(1), P. 301–305.
[16] Sun Y., Yang S., Zhang Y., Jiang J., Jiang H. Coprecipitation synthesis of gadolinium aluminum gallium oxide (GAGG) via different precipitants. *IEEE Trans. Nucl. Sci.*, 2014, **61**(1), P. 306–311.
[17] Zhang J., Luo Z., Jiang H., Jiang J., Gui Z., Chen C., Ci M. Sintering of GGAG:Ce^{3+}, xY^{3+} transparent ceramics in oxygen atmosphere. *Ceram. Int.*, 2017, **43**(17), P. 16036–16041.
[18] Korzhik M., Alenkov V., Buzanov O., Fedorov A., Dosovitskiy G., Grigorjeva L., Mechinsky V., Sokolov P., Tratsiak Y., Zolotarjovs A., Dormenev V., Dosovitskiy A., Agrawal D., Anniyev T., Vasilyev M., Khabashesku V. Nanoengineered $Gd_3Al_2Ga_3O_{12}$ scintillation materials with disordered garnet structure for novel detectors of ionizing radiation. *Cryst. Res. Technol*, 2019, **54**(4), P. 1800172.
[19] Lamoreaux H., Hildenbrand D., Brewer L. High-temperature vaporization behavior of oxides II. Oxides of Be, Mg, Ca, Sr, Ba, B, Al, Ga, In, Tl, Si, Ge, Sn, Pb, Zn, Cd, and Hg. *J. Phys. Chem. Ref. Data*, 1987, **16**(3), P. 419–443.
[20] Dosovitskiy G., Karpyuk P., Evdokimov P., Kuznetsova D., Mechinsky V., Borisevich A., Fedorov A., Putlayev V., Dosovitskiy A., Korjik M. First 3D-printed complex inorganic polycrystalline scintillator. *CrystEngComm*, 2017, **19**(30), P. 4260–4264.
[21] Dosovitskiy G., Dubov V., Karpyuk P., Volkov P., Tamulaitis G., Borisevich A., Vaitkevičius A., Prikhodko K., Kutuzov L., Svetogorov R., Veligzhanin A., Korzhik M. Activator segregation and micro-luminescence properties in GAGG:Ce ceramics. *J. Lumin.*, 2021, **236**, P. 118140.
[22] Dosovitskiy G., Dubov V., Karpyuk P., Volkov P., Tamulaitis G., Borisevich A., Vaitkevičius A., Prikhodko K., Kutuzov L., Svetogorov R., Veligzhanin A., Korzhik M. Activator segregation and micro-luminescence properties in GAGG:Ce ceramics. *J. Lumin.*, 2021, **236**, P. 118140.
[23] Kirkin R., Mikhailin V., Vasil'ev A. Recombination of correlated electron-hole pairs with account of hot capture with emission of optical phonons. *IEEE Trans. Nucl. Sci.*, 2012, **59**, P. 2057–2064.
[24] Vasil'ev A., Korzhik M., Gektin A. Microtheory of scintillation in crystalline materials. *Eng. Scint. Mat. Rad. Technol.: Proc. ISMART – Springer Int. Publ.*, 2017, P. 3-34.
[25] Korzhik M., Tamulaitis G., Vasil'ev A. *Physics of Fast Processes in Scintillators*. Cham : Springer, 2020, **262**, P. 250.
[26] Vasil'ev A., Gektin A. Multiscale Approach to Estimation of Scintillation Characteristics. *IEEE Trans. Nucl. Sci.*, 2014, **61**, P. 235–245.

Submitted 13 November 2024; revised 25 November 2024; accepted 30 November 2024

Information about the authors:

Valentina G. Smyslova – National Research Center "Kurchatov Institute", Moscow, 123182, Russian Federation; ORCID 0000-0001-8475-2602; smyslovavg@gmail.com; smyslova_vg@nrcki.ru

Vasiliy M. Retivov – National Research Center "Kurchatov Institute", Moscow, 123182, Russian Federation; ORCID 0000-0002-3649-2778; vasilii_retivov@mail.ru

Valery V. Dubov – National Research Center "Kurchatov Institute", Moscow, 123182, Russian Federation; ORCID 0000-0002-5816-1582; valery_dubov@mail.ru

Lidia V. Ermakova – National Research Center "Kurchatov Institute", Moscow, 123182, Russian Federation; ORCID 0000-0001-7263-5724; ermakova_lv@nrcki.ru

Vladimir K. Ivanov – Kurnakov Institute of General and Inorganic Chemistry, Moscow, 119071, Russian Federation; ORCID 0000-0003-2343-2140; van10@mail.ru

Petr V. Karpyuk – National Research Center "Kurchatov Institute", Moscow, 123182, Russian Federation; ORCID 0000-0003-0002-3483; karpyuk_pv@nrcki.ru

Ilya Yu. Komendo – National Research Center "Kurchatov Institute", Moscow, 123182, Russian Federation; ORCID 0000-0003-3622-173X; komendo_iyu@nrcki.ru

Daria E. Lelekova – National Research Center "Kurchatov Institute", Moscow, 123182, Russian Federation; ORCID 0000-0001-5538-1726; daria_kyznecova@inbox.ru

Vitaly A. Mechinsky – National Research Center "Kurchatov Institute", Moscow, 123182, Russian Federation; "Institute for Nuclear Problems" of the Belarusian State University, Minsk, 220030, Republic of Belarus; vitaly.mechinsky@gmail.com

Andrey N. Vasil'ev – Skobeltsyn Institute of Nuclear Physics, Moscow State University, Moscow, 119234, Russian Federation; anv@sinp.msu.ru

Artemii S. Ilyushin – Skobeltsyn Institute of Nuclear Physics, Moscow State University, Moscow, 119234, Russian Federation; ORCID 0009-0007-0850-988X; artyom2833@mail.r

Petr S. Sokolov – National Research Center "Kurchatov Institute", Moscow, 123182, Russian Federation; ORCID 0000-0003-3516-3953; sokolov_ps@nrcki.ru

Mikhail V. Korzhik – National Research Center "Kurchatov Institute", Moscow, 123182, Russian Federation; "Institute for Nuclear Problems" of the Belarusian State University, Minsk, 220030, Republic of Belarus; korjikmikhail@gmail.com
Conflict of interest: the authors declare no conflict of interest.